Numerical Predictions of the Unburned Gas Flow Field Ahead of a Flame Propagating in an Obstructed Channel using Large Eddy Simulation

Craig Johansen and Gaby Ciccarelli,

Department of Mechanical and Materials Engineering, Queen's University, Kingston, Canada

1 Introduction

Recent advances in computing technology have made it possible to further investigate complex combustion problems such as flame acceleration in an obstructed channel [1]. A recent study by Johansen and Ciccarelli [2] investigated the unburned gas flow field generated ahead of an accelerating flame using high-speed schlieren photography. In the experiment, the flame is ignited at one end of a closed channel via a weak spark. The expansion of the combustion products induces a flow in the unburned gas ahead of the flame front. The unburned gas flows over rectangular obstacles mounted to the top and bottom channel walls producing a transverse velocity gradient, see Fig. 1. As the flame propagates into this region, convection of the flame surface results in an increase in flame area. The corresponding increase in volumetric burning rate results in the acceleration of the flame front. Via a visualization technique using injected helium tracer gas, the structure of the unburned gas flow field for tests with a range obstacle blockage ratios (BR) were obtained. This technique, illustrated in Fig. 1, involves injecting a finite amount of helium gas into a pocket between obstacles prior to ignition. Due to the density gradient associated with the methane-air/helium gas interface, schlieren images are able to reveal the structure of the vortex that forms downstream of the obstacle.

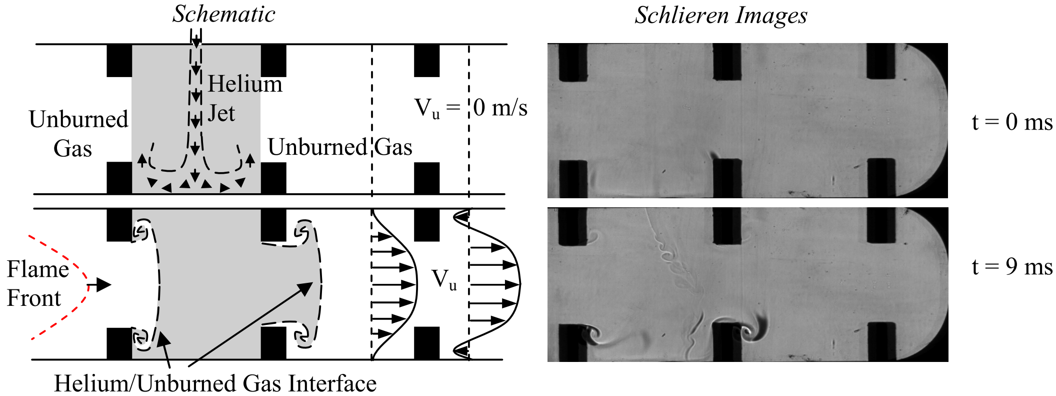

Figure 1: Helium injection visualization technique [2]

Correspondence to: johansen@me.queensu.ca

In this study, the convection of this helium pocket is numerically simulated in order to further understand the development of the unburned gas flow field into which the flame front propagates. Most numerical investigations associated with flame acceleration have been restricted to two dimensional simulations due to the large computational resources required [1]. However, by restricting the simulation to early stages of the flame acceleration, it is possible to investigate the three dimensional nature of the vortex rollup process, which is not available from the experiment.

2 Numerical Model

A compressible Large Eddy Simulation (LES) of the unburned gas flow field ahead of the flame front was undertaken using the commercial code Fluent 6.3, and was run on twelve UltraSPARC-IV, 1.5GHz processors at the Canadian High Performance Computing Virtual Laboratory (HPCVL). The computational domain shown in Fig. 2a includes a mass flux inlet, periodic boundaries on the sides, no-slip top and bottom walls, and a pressure outlet. The specification of the mass flux inlet was obtained experimentally [2] by tracking the convection of the methane-air/helium gas interface across the top of the obstacle surface. An exponential equation was curve fitted to this data and extrapolated to obtain the mass flux at later times. For stoichiometric methane-air at an initial pressure of P_i = 47 kPa and initial density of ρ_u = 0.535 kg/m^3, the unsteady mass flux, $\dot{m}$, is specified as:

$$\dot{m} = A\rho_u t^n \tag{1}$$

where t is time and A and n are empirical constants with values of 12,400 and 1.7, respectively.

Subgrid viscosity in the simulations is calculated using the standard Smagorinsky Subgrid Model [3]. The convection of a passive scalar initialized to a value of c = 1 upstream of the second obstacle allows for the visualization of the methane-air/helium interface observed in the experiment. The obstacle spacing in Fig. 2a is equal to the channel height of H = 7.62 cm and the length of the computational domain is L/H = 1.5. The domain width was varied from a pure 2D simulation to a maximum width of W/H = 0.67. The channel width in the experiment is W/H = 1. The base grid has a node spacing of Δ = 0.6 mm, which corresponds to H/Δ = 128 and a total of one million nodes in the entire domain. High aspect ratio volumes near wall surfaces ensured a wall y^+ less than one. A sensitivity study of the domain length and width reveals that early vortex development before the shear layer spans the distance between obstacles is predominately two dimensional and independent of total domain length.

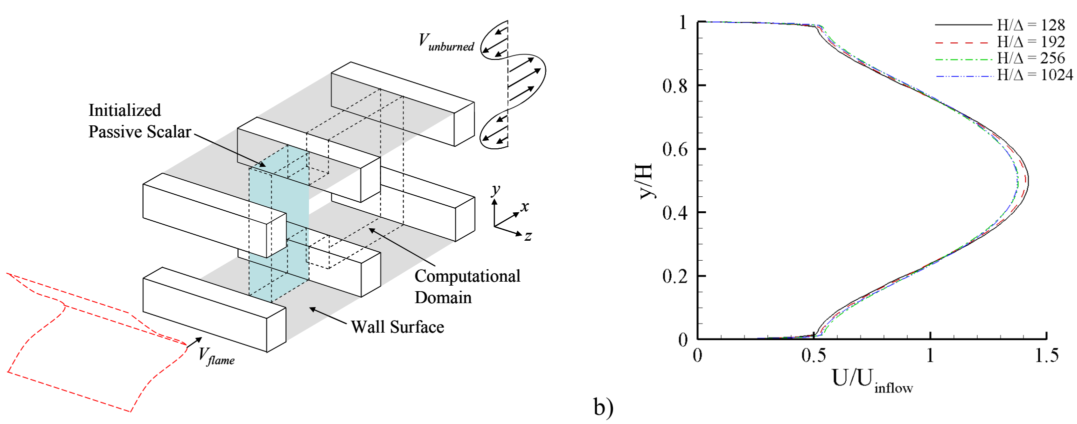

a) b)

Figure 2: a) computational domain and b) grid sensitivity (BR = 0.5, W/H = 0.67)

In addition to domain shape, solution sensitivity to grid resolution was also investigated, which is shown in Fig. 2b. The base grid was uniformly reduced to Δ = 300 μm and 75 μm using grid adaptation, where grid volumes are dynamically refined based on the local gradient of mass fraction, wall y+, and strain rate. Although smaller grid spacing allows for finer flow structures to be resolved, the global development of the velocity field appears to be unaffected by the increased resolution.

3 Simulation Results

Figure 3 shows the three-dimensional vortex development downstream of the first obstacle in the domain. This is done by tracking the c = 0.5 isosurface of the passive scalar over time. This surface shows the two-dimensional development of the recirculation zone downstream of an obstacle. However, after the recirculation zone spans the distance between obstacles (t = 20 ms), span-wise variations along the isosurface are observed as the flow field starts to become three-dimensional. Contours of x-vorticity in subsequent y-z planes (not shown in Fig. 3) show small scale vortical structures occurring in the streamwise direction. Stream-traces distributed near the bottom channel surface indicate that for early simulation times (t = 13.3 ms) the flow field contracts and expands past obstacles. This oscillating streamwise velocity is responsible for the oscillating flame tip velocity observed in the experiment. However, at later times (t = 20 ms) the shear layer that develops spans the distance between obstacles and stream-traces appear be parallel. Large deformations along the c isosurface are due to the interaction with the discreet vortices that are a shed along the shear layer. This is observed as small clumps of z-vorticity shown on the x-y plane on the left periodic boundary.

The c isosurface is colored with contours of subgrid viscosity ratio. Low levels (blue color) of subgrid viscosity were observed along the shear layer and within the core flow between the obstacles. As expected the largest levels (red color) of subgrid viscosity were observed near the leading edge of each obstacle where the level of strain rate was the maximum. At t = 20 ms, the level of subgrid viscosity exceeds five times the magnitude of the molecular viscosity and span-wise variations begin to occur in the c isosurface. Simulation times beyond t = 20 ms cannot be compared directly to experiments since the flame front enters the field of view and largely affects the flow field. Experiments with helium injection place further downstream from the ignition point would accommodate longer unburned gas flow development; however a longer computational domain would be required for accurate predictions.

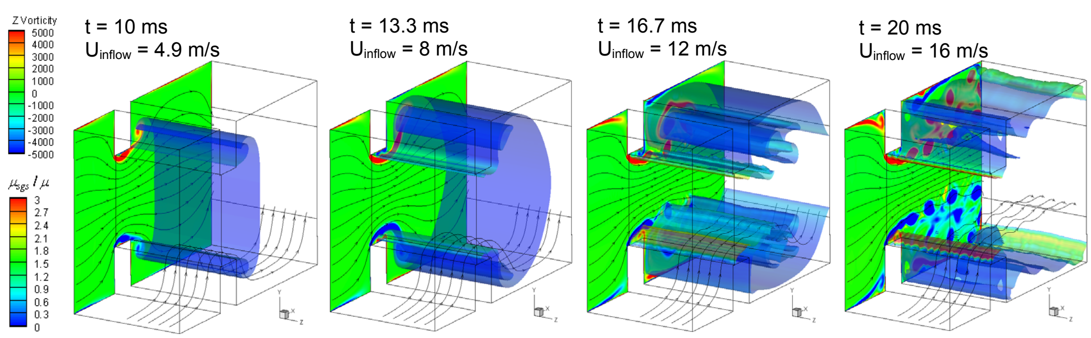

Figure 3: Predictions of 3D flow field development for 0.5 BR obstacles, domain width = 0.67H

One of the main objectives of this study is to understand the effect of obstacle blockage ratio on the unburned gas flow field. Qualitatively, Fig. 4a shows the convection of the passive scalar, c, for three different blockage ratios and is compared to the methane-air/helium gas interface observed in the experimental schlieren images. The inflow boundary condition is identical for each of the simulations corresponding to their respective obstacle BR. The early flow development is predicted extremely well however, it appears that the size of the shear layer vortices predicted by the simulations is much larger than what is observed in the experiment. Fig. 4b shows the evolution of centerline streamwise velocities for three simulation times. The smooth sinusoidal oscillation in centerline velocity observed during the early laminar development of the recirculation zone, e.g., up to 10 ms, is broken by the shedding of vortices from the leading edge of the obstacle surface, e.g., 20 ms.

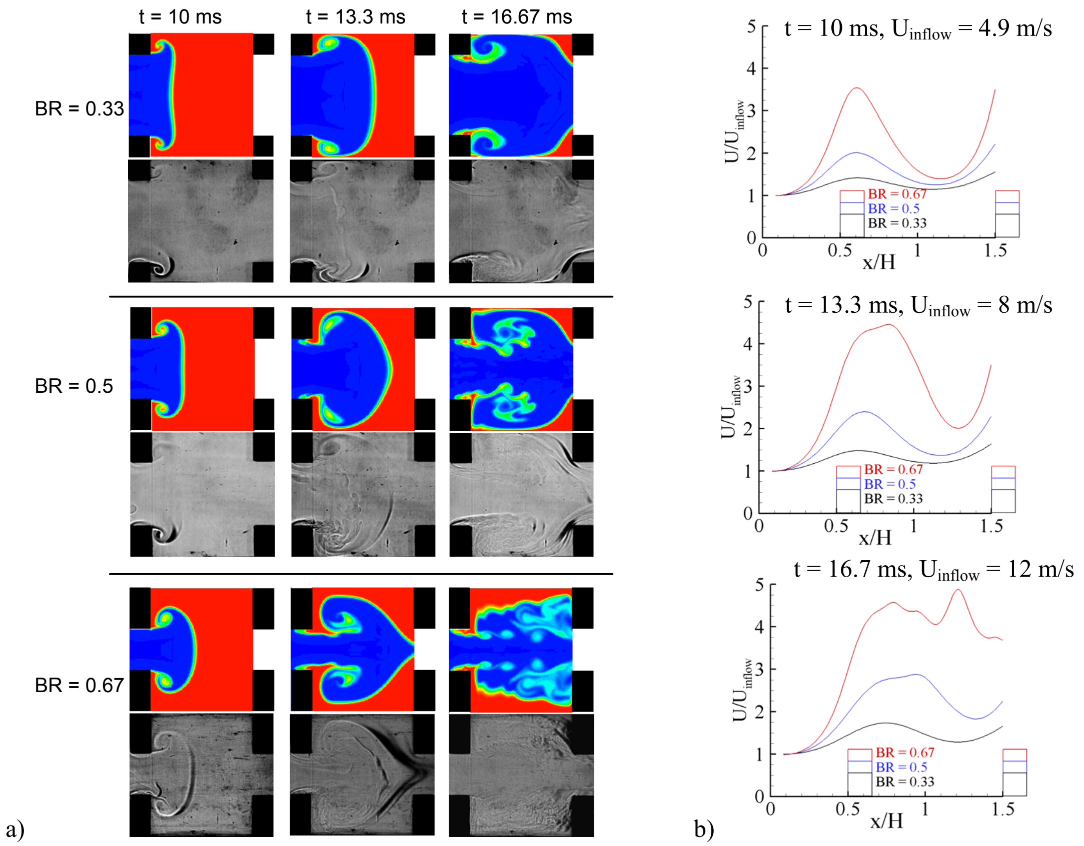

Figure 4: Effect of blockage ratio on flow field development shown in a) development of the helium/methane air interface and b) profiles of centerline streamwise velocity

4 Conclusions

Numerical predictions indicate a transition from 2D to 3D flow as the recirculation zones grow to span the distance between obstacles. This point corresponds to high levels of subgrid viscosity produced near the obstacle leading edge and to the shedding of vortices within the shear layer. The flame front velocity oscillations that are observed in experiments can be accounted for by the expansion and contraction of the flow field predicted by the model. The model prediction also indicates that the observed late-time flame front velocity oscillations are not caused by flow contraction and expansion.

References

[1] Gamezo V., Takanobu O., Oran, E. (2007) Effects of obstacle spacing on flame acceleration in obstructed channels, 21st ICDERS, Poitier.

[2] Johansen C. and Ciccarelli G. (2008) Visualization of the unburned gas flow field ahead of an accelerating flame in an obstructed square channel, Combustion and Flame (DOI: 10.1016/j.combustflame.2008.07.01).

[3] Smagorinsky J. (1963) General circulation experiments with the primitive equations: I. the basic experiment, Monthly Weather Review, 91: 99-164.